© creative

Scientific paper

Synthesis, Labeling and Biological Evolution of New Thiopyrano[2,3-b]Pyridine Derivatives as Potential Anticancer Agents

Mamdouh Abdel-Monem Sofan,^{1,*} Wafaa Salama Hamama,² Ibrahim Ibrahim EL-Hawary,¹ Ismail Taha Ibrahim³ and Hanafi Hassan Zoorob²

¹ Chemistry Department, Faculty of Science, Damietta University, Egypt

² Chemistry Department, Faculty of Science, Mansoura University, Egypt

³ Hot Laboratories Center, Atomic Energy Authority, Cairo, Egypt

* Corresponding author: E-mail: masofan1953@du.edu.eg

Received: 01-12-2019

Abstract

The new thiopyrano[2,3-b]pyridines 4–9 could be synthesized from the nicotinonitrile derivative 1. The cytotoxicity activity of the selected compounds 5, 6 and 8 was tested against MCF-7 and HCT-116 cell lines. The compound 5 (TP₅) exhibited significant inhibitory activity and displayed the most potent activity, more than 6 and 8. The compound 5 with potent inhibitory activity in tumor growth inhibition would be a potential anticancer agent. In the light of this result, the labeled 125 I-compound 5 (125 I-TP₅) was prepared and its cytotoxicity against ascites tumor in mice has been evaluated. The results show that compound 5 (TP₅) may be potentially used as a radiopharmaceutical for tumor diagnosis when labeled with 125 I.

Keywords: Nicotinonitrile; thiopyrano[2,3-*b*]pyridine; cytototoxic activity; ascites tumor.

1. Introduction

Cancer is one of the main leading causes of death in both developing and developed countries. Cancer treatment has been a major research and development effort in academia and the pharmaceutical industry for numerous years.^{2,3} Despite the fact that there is a large amount of information available dealing with the clinical aspects of cancer chemotherapy, there was a clear requirement for an updated treatment from the point of view of medicinal chemistry and drug design. Another major goal for developing new anticancer agents is to overcome cancer resistance to drug treatment, which has made many of the currently available chemotherapeutic agents ineffective.⁵ The pyridine nucleus is an integral part of anti-inflammatory and anticancer agents.^{6,7} Some of 4-oxothiopyrano[2,3-b] pyridines were reported as potential antihypertensive agents.^{8,9} α,β-Unsaturated compounds have also exhibited excellent antitumor, anti-inflammatory, antimalarial and

other pharmacological effects. $^{10-13}$ In recent years, the synthesis and antifungal activities of 3-substituted methylene-4-oxothiopyrano [2,3-b] pyridines were published. 14,15 A number of the spiropyrazolo-3,3'-thiopyrano [2,3-b] pyridines and new tetra- and penta-heterocycles, which could be obtained by treating 3-(N,N-dimethylamino) methylene derivatives with nitrilimines and aminoazoles, respectively, showed high antifungal and anti-bacterial activities. 15

Motivated by the above literature observations and our own previous reports, ^{16–18} herein we describe the use of the 4,6-dimethylnicotinonitrile-2-thiol (1) for the synthesis of thiopyranopyridine heterocyclic ring systems (Schemes 1–3) to investigate their antitumor activities. In addition, we were able to perform the iodine labeling of the new compound 5 using NBS as an oxidizing agent and examined the factors affecting the labeling yield. Bio-distribution of the labeled compound in normal and ascites bearing mice was also studied.

2. Experimental

2. 1. Synthesis Procedures of the New Compounds

All melting points are uncorrected and were determined on Gallenkamp electric melting point device. The completion of the reactions and the purity of the compounds were determined by TLC on silica gel pre-coated aluminum sheets (Type 60 F254, Merck, Darmstadt, Germany) and spots were visualized under UV light (254 nm). The infrared (IR) spectra were recorded on a Jasco 4100 FTIR spectrophotometer as KBr discs (v_{max} in cm⁻¹). ¹H NMR spectra were recorded on a Bruker Avance 400 spectrometer operating at 400 MHz and ¹³C NMR spectra on the same instrument at 75 MHz. Deutrated DMSO- d_6 was used as the solvent, tetramethylsilane (TMS) was used as the internal standard and chemical shifts were measured on δ scale, given in ppm. The mass spectra were recorded on a Shimadzu GCMS-QP 1000 EX mass spectrometer at 70 eV. Elemental analyses were performed on Perkin-Elmer 2400 elemental analyzer at the Micro-analytical Center at Cairo University, Cairo, Egypt.

Synthetic Procedure for Ethyl 3-(3-Cyano-4,6-dimethylpyridin-2-ylthio)propanoate (2)

A mixture of compound 1 (3.28 g, 0.02 mol), ethyl bromopropanoate (3.6 g, 0.02 mol) and sodium carbonate (2.12 g, 0.02 mol) in DMF (50 mL) was heated under reflux with stirring for 4 h. The mixture was left to cool to room temperature, poured into water (50 mL), extracted with dichloromethane (3×50 mL). The organic layer was dried over anhydrous sodium sulfate, filtered off, and the solvent was stripped under vacuum. The precipitate formed was dried and recrystallized from methanol to give compound 2 (4.2 g, 80%).

White powder; mp 77–78 °C; IR (KBr): v/cm^{-1} 2215.81 (CN); 1727.91 (CO, ester); ¹H NMR (400 MHz, DMSO- d_6) δ (ppm) 1.29 (t, 3H, CH₃-ester), 2.50 (s, 3H, CH₃-4), 2.53 (s, 3H, CH₃-6), 2.82 (t, 2H, CH₂-CO), 3.50 (t, 2H, CH₂-S), 4.18 (q, 2H CH₂-O, ester), 6.85 (s, 1H, C₅-H pyridine); ¹³C NMR (75 MHz, DMSO- d_6) δ (ppm) 14.43, 20.35, 25.44, 25.94, 34.65, 60.95, 108.09, 115.71, 120.74, 152.15, 161.61, 161.62, 172.03; MS (El, 70 eV) $m/z = 264(\text{M}^+)$. Anal. Calcd for C₁₃H₁₆N₂O₂S (264.09): C, 59.07; H, 6.10; N, 10.60. Found: C, 60.54; H, 6.19; N, 10.75.

Synthetic Procedure for Ethyl 3,4-Dihydro-5,7-dimethyl-4-oxo-2H-thiopyrano[2,3-b]pyridine-3-carboxylate (3)

A solution of 2 (2.64 g, 0.01 mol) in THF (25 mL) was added dropwise to sodium hydride (1.2 g, 60%, 0.03 mol) in THF (50 mL) during 30 min with stirring under nitrogen at room temperature. The reaction mixture was heated under reflux for 6 h and left to cool to room temperature. After cooling in an ice bath, absolute ethanol (10 mL) was dropwise added and then cold water (50 mL). Af-

ter neutralization, to the mixture diluted HCl (50 %) was added, it was extracted with dichloromethane (3×50 mL). The organic layer was dried over anhydrous sodium sulfate, filtered off and the solvent was removed in vacuum. The solid residue was triturated with water and the precipitate formed was filtered, dried and recrystallized from ethanol to give title compound 3 (1.9 g, 72%).

Yellowish powder; mp 80–81 °C; IR (KBr): ν /cm⁻¹ 1714.3 and 1666.2 (2 × C=O). ¹H NMR (400 MHz, DMSO- d_6) δ (ppm) 1.30 (t, 3H, CH₃- ester), 2.52 (s, 3H, CH₃-5), 2.58 (s, 3H, CH₃-7), 2.78 (d, 2H, CH₂-2), 4.28 (q, 2H, CH₂-ester), 5.41 (br., 1H, C₃-H), 7.19 (s, 1H, C₆-H); ¹³C NMR (75 MHz, DMSO- d_6) δ (ppm) 14.29, 20.02, 22.48, 38.81, 40.06, 60.12, 122.26, 123.30, 147.66, 149.56, 157.25, 158.02, 164.50; MS (El, 70 eV) $m/z = 265(M^+)$. Anal. Calcd for C₁₃H₁₅NO₃S (265.11): C, 58.85; H, 5.70; N, 5.28. Found: C, 58.18; H, 5.32; N, 5.22.

Synthetic Procedure for 2,3-Dihydro-5,7-dimethylthio-pyrano[2,3-b]pyridin-4-one (4)

A solution of β -ketoester 3 (1.25 g, 0.005 mol) in acetic acid (20 mL) and conc. HCl (10 mL) was heated under reflux for 4 h. After cooling to room temperature, the mixture was poured into cold water and solid formed was filtered off. This solid was left to dry and recrystallized from methanol to give the pure product 4 (0.7 g, 80%).

White powder; mp 95–96 °C; IR (KBr): v/cm^{-1} 1666.8 (CO). ¹H NMR (400 MHz, DMSO- d_6) δ (ppm) 2.51(s, 3H, CH₃-3), 2.53 (s, 3H, CH₃-7), 3.33 (t, 2H, CH₂-2), 3.01 (t, 2H, CH₂-3), 7.11 (s, 1H, C₆-H pyridine); ¹³C NMR (75 MHz, DMSO- d_6) δ (ppm) 19.00, 23.29, 24.99, 40.01, 118.91, 128.02, 145.01, 158.34, 161.99, 195.10; MS (El, 70 eV) $m/z = 193(\text{M}^+)$. Anal. Calcd for C₁₀H₁₁NOS (193.06): C, 62.15; H, 5.74; N, 7.25. Found: C, 62.10; H, 5.79; N, 7.28.

Synthetic Procedure for Ethyl 2-(3,4-Dihydro-5,7-dimethyl-4-oxo-2H-thiopyrano[2,3-b]pyridin-3-yl)-2-oxoacetate (5)

A mixture of thiopyranopyridin-4-one **4** (1.93 g, 0.01 mol) with diethyl oxalate (1 mL) in ethanol (20 mL) in the presence of sodium ethoxide was heated with stirring for 3 h. After cooling, the reaction mixture was poured into ice-cold water, acidified with dil. HCl. The formed precipitate was filtered off, dried and recrystallized from aqueous ethanol to give compound **5** (2.37 g, 81%).

White powder; mp 99–100 °C; IR (KBr): ν /cm⁻¹ 1714.3 and 1666.2 (CO); ¹H NMR (400 MHz, DMSO- d_6) δ (ppm) 1.29 (t, 3H, CH₃-ester), 2.52 (s, 3H, CH₃-5), 2.58 (s, 3H, CH₃-7), 2.78 (s, 2H, CH₂-2), 4.29 (2H, q, CH₂, ester), 5.41 (br., 1H, C₃-H), 7.19 (H, s, CH-6); ¹³C NMR (75 MHz, DMSO- d_6) δ (ppm) 14.29, 20.03, 22.48, 60.13, 38.81, 94.12, 122.26, 123.30, 147.66, 149.56, 157.25, 158.02, 164.51; MS (El, 70 eV) m/z = 293 (M⁺). Anal. Calcd for C₁₄H₁₅NO₄S (293.07): C, 57.32; H, 5.15; N, 4.77. Found: C, 57.39; H, 5.22; N, 4.70.

Synthetic Procedure for 5',7'-Dimethyl-2',3'-dihydrospiro[imidazolidine-4,4'-thiopyrano[2,3-b]pyridine]-2,5-dione (6)

A mixture of compound 4 (1.93 g, 0.01 mol), potassium cyanide (0.975 g, 0.015 mol) and ammonium carbonate (0.5 g) was dissolved in 30 mL of water – ethanol (2:1) solution. The reaction mixture was heated under reflux at 60 °C for 48 h. The reaction mixture was kept in refrigerator overnight. The formed precipitate was filtered off, dried and recrystallized from aqueous ethanol to give compound 6 (2.26 g, 86%).

White powder; mp 91–92 °C; IR (KBr): v/cm^{-1} 3414.3 (NH) and 1666.2 (CO); ¹H NMR (400 MHz, DMSO- d_6) δ (ppm) 2.42 (s, 3H, CH₃-5'), 2.50 (s, 3H, CH₃-7'), 2.99 (t, 2H, CH₂-3'), 3.50 (t, 2H, CH₂-2'), 6.69 (s, 1H, NH-3), 7.15 (s, 1H, CH-6'), 13.80 (s, 1H, NH-1); ¹³C NMR (75 MHz, DMSO- d_6) δ (ppm) 17.57, 18.73, 19.58, 25.08, 104.13, 116.15, 120.69, 152.49, 156.75, 159.26, 161.61, and and 177.42; MS (El, 70 eV) m/z = 263 (M⁺). Anal. Calcd for C₁₂H₁₃N₃O₂S (263.07): C, 54.74; H, 4.98; N, 15.96. Found: C, 54.70; H, 4.91; N, 15.90.

Synthetic Procedure for (Z)-3-((Dimethylamino)methylene)-2,3-dihydro-5,7-dimethylthiopyrano[2,3-b]pyridine-4-one (7)

A mixture of precursor 4 (1.93 g, 0.01 mol) with DMFDMA (1 mL) in dioxane (20 mL) in the presence of freshly prepared sodium ethoxide (0.23 g in 0.66 mL of absolute ethanol) was heated with stirring for 3 h. After cooling to room temperature, the reaction mixture was poured into ice-cold water then the formed precipitate was filtered off, dried and recrystallized from aqueous ethanol to give compound 7 (1.9 g, 77%).

White powder; mp 76–77 °C; IR (KBr): v/cm^{-1} 1666.2 (CO). ¹H NMR (400 MHz, DMSO- d_6) δ (ppm) 2.41(s, 3H, CH₃), 2.54 (s, 3H, CH₃), 3.23 (m, 6H, N(CH₃)₂), 3.28 (s, 2H, CH₂-2), 6.41 (s, 1H, CH-6), 7.27 (s, 1H, =CH); ¹³C NMR (75 MHz, DMSO- d_6) δ (ppm) 17.59, 24.07, 43.55, 28.9, 111.73, 181.16, 120.43, 125.30, 142.48, 160.48, 162.95; MS (El, 70 eV) m/z = 248 (M⁺). Anal. Calcd for C₁₃H₁₆N₂OS (248.10): C, 62.87; H, 6.49; N, 11.28. Found: C, 62.80; H, 6.42; N, 11.23.

Synthetic Procedure for (Z)-3-(Ethoxymethylene)-2,3-dihydro-5,7-dimethylthiopyrano[2,3-b]pyridine-4-one (8)

A mixture of compound 4 (1.93 g, 0.01 mol) with triethyl orthoformate (1 mL) in DMF (20 mL) was heated with stirring for 3 h in the presence of piperdine as the catalyst. The reaction mixture was left overnight at room temperature, poured into ice-cold water and acidified with dil. HCl. The formed precipitate was filtered off, dried and recrystallized from aqueous ethanol to give compound 8 (1.69 g, 68%).

Yellow powder; mp 86–87 °C; IR (KBr): v/cm^{-1} 1714.3 (CO- ester) and 1666.2 (CO). ¹H NMR (400 MHz, DMSO- d_6) δ (ppm) 1.23 (t, 3H, CH₃- ester), 2.52 (m, 6H,

2CH₃), 3.65 (s, 2H, S-CH₂), 4.11 (q, 2H, CH₂- ester), 6.51 (s, 1H, O-CH), 6.93 (s, 1H, pyridyl); 13 C NMR (75 MHz, DMSO- d_6) δ (ppm) 15.39, 17.86, 23.04, 26.54, 62.83, 107.21, 120.69, 126.11, 142.45, 160.92, 163.02, 162.7, 179.85; MS (El, 70 eV) m/z = 249 (M⁺). Anal. Calcd for C₁₃H₁₅NO₂S (249.08): C, 62.62; H, 6.06; N, 5.62. Found: C, 62.68; H, 6.01; N, 5.67.

Synthetic Procedure for 2,7,9-Trimethyl-2,4-dihydropyr-azolo[3',4':4,5]thiopyrano[2,3-b]pyridine (9)

A mixture of 7 (2.48 g, 0.01 mol) and/or 8 (2.49 g, 0.01 mol) with methylhydrazine (0.46g, 2 mL, 0.01 mol) in DMF (20 mL) was stirred for 1 h. The reaction mixture was heated under reflux for 4 h. The reaction mixture was left to cool to room temperature and poured into ice-cold water. The formed precipitate was filtered off, dried and recrystallized from ethanol to give compound 9 (1.57 g, 68%).

Yellow powder; mp 77–78 °C; 1 H NMR (400 MHz, DMSO- d_6) δ (ppm) 2.53 (s, 3H, CH₃-9), 2.58 (s, 3H, CH₃-7), 3.87 (s, 3H, CH₃-2), 4.29 (s, 2H, S-CH₂), 6.56 (s, 1H, CH-8), 7.93 (s, 1H, CH-3); 13 C NMR (75 MHz, DMSO- d_6) δ (ppm) 18.73, 21.54, 40.36, 23.69, 116.01, 118.10, 128.36, 131.10, 145.16, 156.00, 160.09; MS (El, 70 eV) m/z = 231 (M⁺). Anal. Calcd for C₁₂H₁₃N₃S (231.32): C, 62.31; H, 5.66; N, 18.17. Found: C, 62.39; H, 5.72; N, 18.11.

2. 2. Cytotoxic Activity

2. 2. 1. Determination of the Anticancer Activity

Material and Method: (i) MCF-7 (Breast Carcinoma Cell Line) (ii) HCT-116 (Colon Carcinoma Cell line).

Measurement of Potential Cytotoxicity:

The potential cytotoxicity of the tested compounds was evaluated using the MTT assay. The cell lines were plated in 96-multiwell plates (10⁴ cells/well) for 24 h before treatment with the prepared compounds to allow the attachment of cells to the wall of the plate. The tested compounds were dissolved in dimethyl sulphoxide (DMSO) and diluted 1000-fold in the assay. Different concentrations of the tested compound were added to the cell monolayer; triplicate wells were prepared for each individual dose. Monolayer cells were incubated with the compounds for 48 h at 37 °C, in atmosphere of 5% CO₂. After 48 h, cells were fixed, washed and stained for 30 min with 0.4% (wt/vol) Sulfo-Rhodamine-B stain (SRB). The excess stain was washed with 1% acetic acid and attached stain was recovered with Tris EDTA buffer. The color intensity was measured in an ELISA reader. The relation between cell viability and drug concentration was plotted to get the survival curve of tumor cell line and the IC50 was calculated. The relation between cell viability, inhibitory effect and drug concentration is shown in Tables 1 and 2.

2. 2. 2. The Cytotoxicity of ¹²⁵I-Compound 5 (Synthesis of ¹²⁵I-TP₅)

Materials. NBS (N-bromosuccinimide) used as oxidizing agent, Aldrich chemical company, Germany. Sodium metabisulfite (Na₂S₂O₅): molar mass 190.107 g/mol, The British drug house (BDH) LTD, England. Chloroform (CHCl₃): molar mass 119.38 g/mol, Merck, Darmstadt, Germany. Sodium chloride (NaCl): molar mass 58.44 g/mol, Adwic, Egypt. Ammonium hydroxide (NH₄OH): 98%, Riedel-De Haen Ag., Seelze (Germany). Ethanol (97%) the British Drug House (BDH) Chemicals LTD, England.

Animals. Female Swiss Albino mice weighing 20–25 g were purchased from the Institute of Eye Research, Cairo, Egypt. The environmental and nutritional conditions were kept constant throughout the experimental period. The mice were kept at room temperature (22 \pm 2 °C) with a 12 h on/off light schedule. Female mice were used in this study because their susceptibility to Ehrlich ascites carcinoma was higher than that of the male mice. 19 Animals were kept with free access to food and water throughout the experiment.

EAC: (Ehrlich ascites carcinoma) cells were obtained from Egyptian national cancer institute, Cairo University. The line was transplanted in mice by intraperitoneal injection of cells derived EAC bearing mice after 10 days post inoculation. The cells were injected intraperitoneally to produce ascites (liquid tumor) in the peritoneal cavity and intramuscularly in the right leg to produce solid tumor and leaving the left leg as control.²⁰

Radioactive Materials: Sodium iodide (Na¹²⁵I) was delivered from Institute of Isotopes Co., Ltd as a carrier free and reluctant free solution, Budapest, Hungary.

Synthetic Procedure for Labeling of Compound 5 (TP_5) Using Na¹²⁵I. The ¹²⁵I-TP₅ was synthesized according to the following procedure: 200 μ L of compound 5 solution (1 mg in 1 mL ethanol) in amber colored V-shaped bottom reaction vial. Then, 100 μ L of freshly prepared NBS solution (1 mg in 1 mL ethanol) was added. Then, 10 μ L of ¹²⁵I (3.7 MBq) was added to the reaction mixture. The pH of the reaction mixture was adjusted to pH 3. The reaction mixture was shaken by electric vortex and left at ambient temperature (25 ± 1 °C) for 15 min, after that 20 μ L of saturated sodium metabisulphite solution (30 mg/ mL, H₂O w/v) was added to inhibit the oxidation of the radioiodide.²¹

Ascending Paper Chromatography: On Whatman paper No. 1 sheet (1.5 cm width and 14 cm length), 2 μ L of the reaction mixture was placed 2.5 cm above the lower edge. For development a fresh mixture of solvent (chloroform, methanol) in a ratio of 9:1 (v/v) was used as the mobile phase. After complete development, the paper sheet was removed, dried and cut into strips. Each strip (1 cm width) was counted in a well type γ -counter where radio iodide (I⁻) remained near the origin ($R_f = 0$ –0.1), while the ¹²⁵I-**TP**₅ moved with the solvent front ($R_f = 0.8$).

Paper Electrophoresis: On Whatman No. 1 paper sheet (1.5 cm width and 48 cm length), 1–2 μL of the reaction mixture was placed 10 cm away from the cathode. Electrophoresis was carried out for 1.5 h at voltage of 300 V using phosphate buffer (0.5 M) as electrolytes source solution. After complete development, the paper was removed, dried, and cut into strips. Each strip (1 cm width) was counted in a well type γ-counter. ²² Free radioiodide and $^{125}\text{I-TP}_5$ moved to different distances away from the spotting point towards the anode depending on the charge and the molecular weight of each one (distance from spotting point = 14 and 2 cm, respectively) as shown in Figure 1.

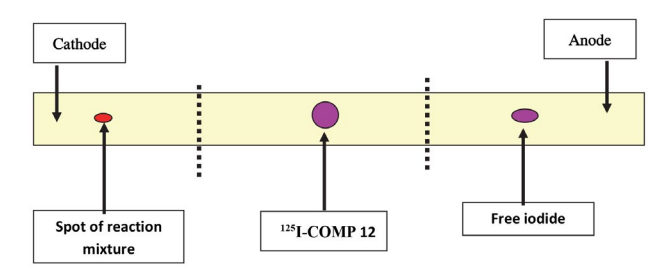


Figure 1: Paper electrophoresis for ¹²⁵I-TP₅ and free iodide.

Factors Affecting the Labeling Yield:

In-vitro Stability of the ¹²⁵I-TP₅. The reaction mixture was prepared at the conditions, which gave the highest radiochemical yield. The mixture was left at ambient temperature and 1–2 μ L samples were taken at different time intervals ranged from 1 up to 24 h. Paper chromatography and electrophoresis was used to determine the *in vitro* stability of the labeled ¹²⁵I-TP₅.

Bio-Distribution Study: Tumor Transplantation in Mice. Ehrlich ascites carcinoma cells (EAC) were one of the excellent models for studying the biological behavior of malignant tumors and drugs assumed to produce effect at these sites. A line of EAC cells was maintained in female Swiss albino mice through weekly IP transplantation of 2.0 \times 10⁶ tumor cells per mouse. EAC cells were obtained by needle aspiration with aseptic condition. The ascetic fluid was diluted with sterile saline so that 0.1 mL contained 2.0 \times 10⁶ cells counted microscopically using a haemocytometer. Thus, 0.2 mL solution was then injected intraperitoneally to produce ascites and intramuscularly in the right thigh to produce solid tumor.²³

General Procedure for Bio-Distribution of the ¹²⁵I-TP₅ in Ascites Bearing Mice. This experiment was carried out using 24 ascites bearing mice. The mice were injected with 0.2 mL (70 KBq) ¹²⁵I-TP₅ in the tail vein and then divided to 4 groups, 6 mice each. The mice were kept in metabolic cages for the recommended times (15, 30, 60 or 180 min) after injection of labeled drug. Mice were sacrificed by cervical dislocation at various time intervals. Organs and tissues of interest were removed, weighted and counted for its uptake of activity. The counting tubes con-

tained a standard equivalent to 100% percent of the injected dose, were assayed in gamma counter and the results were calculated as percentages of injected dose (ID) per gram tissue or organ.²⁴ The weights of blood, bone and muscles were assumed to be 7, 10 and 40 percent of the total body weight, respectively. Ascites were withdrawn using 20 cm plastic syringe, collected, weighted and counted.

General Procedure for Bio-Distribution of the ¹²⁵I-TP₅ in Solid Tumor Bearing Mice. This experiment was carried out using 24 solid tumor bearing mice. Same procedures were done as in ascites bearing mice. In addition tumor muscle was removed and counted for its uptake of activity and compared with that of normal muscle.

3. Result and Discussion

3. 1. Chemistry

The key step in this trial to explore an anticancer drug is the synthesis of 5,7-dimethyl-4-oxothiopyrano[3,4-b]pyridine (4) from 2-mercapto-4,6-dimethylnicotinonitrile (1). Thus, refluxing of the starting material 1 with ethyl 3-bromopropanoate in DMF as a solvent and sodium carbonate afforded the *S*-alkylated derivative 2. The IR spectrum of 2 revealed the presence of the absorption bands for CN and ester's CO functional groups at 2215.81 and 1727.91 cm⁻¹, respectively. While its ¹H NMR indicated the presence of ethyl ester protons at δ 1.29 and 4.18 ppm and the propyl protons at δ 2.82 and 3.50 ppm. Cyclization of 2 by sodium hydride in tetrahydrofuran as a

solvent, followed by an acidic hydrolysis for the imine intermediate produced the corresponding thiopyrano[2,3-b] pyridine 3 in quantitative yield. The $^1\mathrm{H}$ NMR spectrum data for compound 3 declared the presence of ethyl ester protons at δ 1.30 and 4.28 ppm. Its IR spectrum also showed the presence of the absorption bands due to the ester and cyclic ketonic carbonyl groups at 1714.3 and 1666.2 cm $^{-1}$, respectively. The acidic hydrolysis of 3 led to the formation of the cyclic ketone 4 as a target precursor to synthesize the new thiopyranopyridines of pharmaceutical interest. The IR spectrum of 4 indicated the disappearance of the ester's CO group, while $^{1}\mathrm{H}$ NMR showed the absence of ester's ethyl group and appearance of the signal of protons of CH $_2$ -3 group at δ 3.01 ppm (Scheme 1).

In turn, the precursor 4 was treated with diethyl oxalate under Clasien reaction conditions to produce the corresponding ethyl 4-oxalothiopyranopyridine derivative 5. The IR spectrum indicated the absorption band of the oxalo-carbonyls at 1714.3 cm⁻¹ as a broad band and ¹H NMR spectrum revealed the signals of the ethyl protons at δ 1.29 and 4.29 ppm. Also, the compound 4 was reacted with potassium cyanide and ammonium carbonate in ethanol under standard conditions of Bucherer-Bergs reaction to get the 5,7'-dimethyl-2,3'-dihydrospiro[imidazolidine-4,4'-thiopyrano[2,3-b]pyridine]-2,5-dione (6). The IR spectrum of **6** revealed the presence of the absorption bands of NH and CO groups at 3414.3 and 1666.2 cm⁻¹. Its ¹H NMR spectrum indicated the presence of the protons signals of the two NH groups at δ 6.69 and 13.80 ppm (Scheme 2).

$$\begin{array}{c} \text{CH}_3 \\ \text{H}_3\text{C} \\ \text{N} \\ \text{SH} \end{array} + \begin{array}{c} \text{COOEt} \\ \text{Br} \\ \text{COOEt} \end{array} \begin{array}{c} \text{Na}_2\text{CO}_3/\text{ DMF} \\ \text{H}_3\text{C} \\ \text{N} \\ \text{S} \end{array} \begin{array}{c} \text{CH}_3 \\ \text{CN} \\ \text{COOEt} \end{array}$$

Scheme 1. Synthesis of compounds 2, 3 and 4.

Scheme 2. Synthesis of compounds 5 and 6.

Scheme 3. Synthesis of compounds 7-9.

The pyrazolothiopyrano[2,3-b]pyridine 9 was obtained by reacting 3-dimethylaminomethylene-2,3-dihydro-5,7-dimethylthiopyrano[2,3-b]pyridine-4-one (7) or 3-ethoxymethylene-2,3-dihydro-5,7-dimethylthiopyrano[2,3-b] pyridine-4-one (8) with methylhydrazine in ethanol. The enamine 7 and the enether 8 were synthesized by condensing the precursor 4 with DMFDMA in dioxane and/ or triethyl orthoformate in DMF, respectively. The structure elucidation was based on elemental analysis and spectral data. The ¹H NMR spectrum of **9** revealed singlet signals of the protons of the CH₂-4 group at δ 4.20 ppm and CH-3 proton at δ 8.97 ppm, in addition to the three methyl groups at δ 2.53, 2.58 and 3.87 ppm. Formation of 9 takes place via the initial addition of the most nucleophilic NH of the methylhydrazine to exocyclic enamine moiety of 7 followed by elimination of dimethyl amine and water molecules¹⁵ (Scheme 3).

3. 2. Cytotoxicity Evaluation against the MCF-7 and HCT-116 Cell Lines

Three selected new compounds 5, 6 and 8 were tested for cytotoxic activity against the MCF-7 (Breast Carci-

noma Cell Line) and **HCT-116** (Colon Carcinoma Cell line) in the Regional Centre for Mycology and Biotechnology, Al-Azher University (Egypt). All new compounds tested were dissolved in DMSO in different concentrations (Tables 1 and 2).

The compound 5 showed a dramatic inhibitory effect on the growth of MCF-7 cell line and IC_{50} was $3.45\pm0.2~\mu g/mL$. Such inhibitory effect was a dose-dependent manner. The same effect was reported when such compound was tested for its ability to inhibit the growth of HCT-116 cell line with $IC_{50}~13.2\pm0.9~\mu g/mL$. The compound 6 displayed moderately potent toxicity against both MCF-7 and HCT-116 cell lines. Its IC_{50} values were 29.43 \pm 1.1 and 44.1 \pm 1.8 $\mu g/mL$, respectively. The inhibitory activities of compound 8 against MCF-7 and HCT-116 cell lines were detected under the experimental conditions with $IC_{50}~235\pm8.9$ and $IC_{50}~305\pm9.2~\mu g/mL$, respectively and showed low potent toxicity against the two cell lines.

The data indicated to the fact that the compound 5 with potent inhibitory activity in tumor growth inhibition would be a potential anticancer agent. The compound 6 has more potent toxicity against both MCF-7 and

Table 1. Cytotoxic activity against	the MCF-7 of	f tested compounds
--	--------------	--------------------

Sample	Sample Compound 5			Compound 6			Compound 8		
Conc. (µg/mL)	Viability %	Inhibitory %	S.D. (±)	Viability %	Inhibitory %	S.D. (±)	Viability %	Inhibitory %	S.D. (±)
500	3.78	96.22	0.16	5.94	94.06	0.28	31.93	68.07	0.95
250	6.32	93.68	0.06	11.73	88.27	0.19	46.28	53.72	1.86
125	10.86	89.32	0.11	20.46	79.54	0.74	78.14	21.86	2.35
62.5	16.41	83.59	0.38	32.89	67.11	0.98	92.36	7.64	0.72
31.25	23.89	76.11	0.26	47.28	52.72	2.34	99.43	0.57	0.14
15.6	30.75	69.25	0.13	69.41	30.59	1.85	100	0	0
7.8	39.43	60.57	0.61	88.75	11.25	0.61	100	0	0
3.9	46.92	53.08	0.89	98.03	1.97	0.15	100	0	0
2	58.17	41.83	1.24	100	0	0	100	0	0
1	74.89	25.11	0.53	100	0	0	100	0	0
0	100	0	0	100	0	0	100	0	0

Inhibitory activity against Breast carcinoma cells was detected under the experimental conditions with IC₅₀ of compound $\mathbf{5} = 3.45 \pm 0.2$; IC₅₀ of compound $\mathbf{6} = 29.3 \pm 1.1$; IC₅₀ of compound $\mathbf{8} = 235 \pm 8.9 \,\mu\text{g/mL}$.

Table 2. Cytotoxic activity against the HCT-116 of tested compounds

Sample	mple Compound 5				Compound 6			Compound 8		
Conc. (µg/mL)	Viability %	Inhibitory %	S.D. (±)	Viability %	Inhibitory %	S.D. (±)	Viability %	Inhibitory %	S.D. (±)	
500	4.86	95.14	0.21	7.43	92.57	0.31	38.60	61.4	2.32	
250	8.97	91.03	0.39	14.68	85.32	0.76	53.19	46.81	0.97	
125	13.45	86.55	0.43	28.12	71.88	0.45	80.72	19.28	0.32	
62.5	20.63	79.37	0.19	40.96	59.04	1.28	97.85	2.15	0.03	
31.25	31.78	68.22	0.64	56.13	43.69	1.37	100	0	0	
15.6	45.60	54.4	1.82	78.28	21.72	0.54	100	0	0	
7.8	59.72	40.28	0.96	91.87	8.13	0.09	100	0	0	
3.9	71.38	28.62	0.34	99.25	0.75	0.11	100	0	0	
2	85.44	14.56	0.12	100	0	0	100	0	0	
1	97.29	2.71	0.05	100	0	0	100	0	0	
0	100	0	0	100	0	0	100	0	0	

Inhibitory activity against Colon carcinoma cells was detected under the experimental conditions with IC_{50} of compound $\bf 5=13.2\pm0.9$; IC_{50} of compound $\bf 6=44.1\pm1.8$; IC_{50} of compound $\bf 8=305\pm9.2~\mu g/mL$.

HCT-116 cell lines when compared to compound **8**. It seems appropriate to further study the compound **6** *in vivo* and *in vitro* using different cancer cell lines.

3. 3. The Cytotoxicity Evaluation of the Compound 5 (TP₅) Labeled with ¹²⁵I (Synthesis of ¹²⁵I-TP₅)

In the light of the above results of cytotoxicity of compounds 5, 6 and 8 it was interesting for us to radiolabel the ethyl 2-(5,7-dimethyl-4-oxo-3,4-dihydro-2*H*-thiopyrano[2,3-b]pyridin-3-yl)-2-oxoacetate (5) and evaluate the cytotoxicity of the produced labeled compound against ascites tumor in mice to complete the aim of this study for exploring a new antitumor drug. Thus, the 125I-compound 5 (125I-TP₅) was synthesized by direct electrophilic substitution with Na125I under oxidative conditions in the presence of NBS. The radiochemical yield of 125I-TP5 was determined using paper chromatography and electrophoresis. The influence of different factors on the labeling yield, such as the substrate content, NBS content, pH, reaction time and reaction temperature must be determined. Each factor was optimized by the trial and error method. Bio-distribution of the ¹²⁵I-TP₅ in normal and ascites bearing mice was also studied.

Results of the Synthesis of ¹²⁵I-TP₅

Effect of substrate amount on the labeling yield of $^{125}I\text{-}TP_5$ using NBS as oxidizing agent at pH 3 was studied and the results are shown in Table 3. The results showed that the radiochemical yield of $^{125}I\text{-}TP_5$ was low (45.5%) at small substrate amount (10 µg) and reached to maximum labeling value (87.9%) at 75 µg of compound 5. At substrate amounts higher than the optimum amounts, the labeling yield reached plateau. This may be attributed to the fact that the yield reaches the saturation value because the entire generated iodonium ions $[I^+]$ in the reaction were captured at concentration of 0.5 mg. 25

Table 3. Effect of TP_5 amount on the % labeling yield of $^{125}\text{I-TP}_5$

TP ₅ (μg)	% Labeled compound	% Free iodide
10	45.5 ± 0.36*	54.5 ± 0.31
25	65.5 ± 0.6 *	34.5 ± 0.6
50	75.1 ± 0.36 *	24.9 ± 0.25
75	$87.9 \pm 0.40*$	12.1 ± 0.35
100	87.5 ± 0.26 *	12.5 ± 0.30
200	$87.1 \pm 0.40*$	12.9 ± 0.35
500	86.7 ± 0.26 *	13.3 ± 0.30

Values represent the mean \pm SEM, n=6 * Significantly different from the initial values using unpaired student's t-test (P<0.05) † Significantly different from the previous values using unpaired student's t-test (P<0.05).

Effect of the oxidizing agent amount (Table 4). Radioiodination of compound 5 has been performed by using NBS as a mild oxidizing agent to transform iodide (I^-) to iodinium ion (I^+), which allows a spontaneous electrophilic substitution on aromatic ring. ²⁶ At low NBS amount (5 µg), the radiochemical yield of ¹²⁵I-**TP**₅ was 53.5%. Low labeling yield was noted at a low NBS concentration apparently because of incomplete oxidation of iodide to iodonium ions. ²⁵ A high radiochemical yield of 87.5% was achieved by increasing the amount of NBS to 50 µg. The

Table 4. Effect of NBS content on the radiochemical yield of ¹²⁵I-TP₅

NBS (µg)	% Labeled compound	% Free iodide
5	53.5 ± 0.40	46.5 ± 0.3
10	78.1 ± 0.40	21.9 ± 0.3
25	$82.2 \pm 0.40*$	17.8 ± 0.3
50	$87.5 \pm 0.50 * †$	12.5 ± 0.75
100	$87.3 \pm 0.04*$	12.7 ± 0.06
200	$81.2 \pm 0.32*$	18.8 ± 0.35

Values represent the mean \pm SEM, n=6 * Significantly different from the initial values using student's t-test (P<0.05). \pm Significantly different from the previous values using student's t-test (P<0.05).

NBS amount above the maximum labeling value led to decrease in the radiochemical yield. This may be due to the formation of undesirable oxidative by-products *via* process such as bromination,²⁷ polymerization and denaturation of this compound. The formation of these impurities may be attributed to the reactivity and quantity of NBS.²⁸ Consequently, the use of optimum concentration of NBS is highly recommended in order to avoid the formation of by-products and to obtain high yield and purity.

Effect of pH. The nature of active oxidizing species of NBS depends on the pH of the medium and the reaction condition.²⁹ The influence of pH of the reaction mixture on the radiochemical yield of ¹²⁵I-**TP**₅ is shown in Table 5.

Table 5. Effect of pH on the radiochemical yield of ¹²⁵I-TP₅

pH value	% Labeled compound	% Free iodide		
1	25.2 ± 0.30*	7 4.8 ± 0.30*		
2	$80.2 \pm 0.30*$	19.5 ± 0.20		
4	$87.7 \pm 0.44*$ †	12.3 ± 0.25		
5	$80.5 \pm 0.20*$ †	19.5 ± 0.4		
7	$75.5 \pm 0.20*\dagger$	24.5 ± 0.4		

Values represent the mean \pm SEM, n=6 * Significantly different from the initial values using unpaired student's t-test (P<0.05) † Significantly different from the previous values using unpaired student's t-test (P<0.05)

Effect of reaction time. The labeling yield is strongly dependent on reaction time in the range from 1 to 60 min.³⁰ It is clear from Table 6 that the radiochemical yield of ¹²⁵I-TP₅ is significantly increased by increasing the reaction time from 1 to 15 min, at which maximum radiochemical yield obtained (87.5%) and was constant till 15 min. Increasing the reaction time beyond 15 min caused slight decrease in the radiochemical yield and this may be due to exposing the substrate to highly reactive NBS for long reaction time which can result in oxidative side reactions.

Table 6. Effect of reaction time on the % labeling yield of 125I-TP5

Time (min)	% Labeled compound	% Free iodide
1	75.5 ± 0.36	24.5 ± 0.55
5	$80.5 \pm 0.5^*$	19.5 ± 0.15
15	$87.5 \pm 0.3^*$	13.5 ± 0.2
30	$84.7 \pm 0.4*$	15.3 ± 0.1
60	$80.1 \pm 0.25*$	19.9 ± 0.15

Values represent the mean \pm SEM, n=6 * Significantly different from the initial values using unpaired student's t-test (P<0.05)

In-vitro **stability of** ^{125}I - TP_5 . It was observed that ^{125}I - TP_5 was stable for at least 3 h and the stability was decreased by time to reach 75.2% at 12 h post labeling (Table 7).

Table 7. In-vitro stability of ¹²⁵I-TP₅

Time (h)	% Labeled compound	% Free iodide
1	85.5 ± 0.36	14.5 ± 0.55
3	$85.1 \pm 0.5*$	14.9 ± 0.15
6	$80.2 \pm 0.3*$	19.8 ± 0.2
12	$75.2 \pm 0.4*$	24.8 ± 0.1

Values represent the mean \pm SEM, n=6 * Significantly different from the initial values using unpaired student's t-test (P < 0.05)

Table 8. Effect of reaction temperature on the % labeling yield of $^{125}\text{I-TP}_5$

Temperature (°C)	% Labeled compound	% Free iodide
25	87.5 ± 0.36	12.5 ± 0.55
40	$87.5 \pm 0.5*$	12.5 ± 0.15
50	$87.5 \pm 0.3*$	12.5 ± 0.2
75	$80.7 \pm 0.4*$	19.3 ± 0.1
80	$65.1 \pm 0.25*$	34.9 ± 0.15

Values represent the mean \pm SEM, n = 6 * Significantly different from the initial values using unpaired student's t-test (P<0.05)

Table 9. Biodistribution of ¹²⁵I-TP₅ in normal mice

Organs &	% inject	% injected dose/gram tissue at different time intervals					
Body fluids	15 min	30 min	60 min	180 min			
Blood	18.0 ± 0.2	11.0 ± 0.5*	5.2 ± 0.3*	1.2 ± 0.03*			
Bone	1.2 ± 0.05	$2.1 \pm 0.03^*$	$3.2 \pm 0.2^*$	0.9± 0.01*			
Muscle	1.3 ± 0.04	2.3 ± 0.04 *	2.7 ± 0.1	$1.1 \pm 0.09^*$			
Liver	7.2 ± 0.3	$9.8 \pm 0.15^*$	$14.2 \pm 0.2^*$	3.7 ± 0.1			
Stomach	2.3 ± 0.9	4.1 ± 0.4	$3.1 \pm 0.16^*$	$1.1 \pm 0.2^*$			
Intestine	4.5 ± 0.50	$6.2 \pm 0.3^*$	$2.7 \pm 0.1^*$	$2.2 \pm 0.03^*$			
Lung	1.2 ± 0.08	$1.1 \pm 0.12^*$	$0.9 \pm 0.2^*$	$1.2 \pm 0.01^*$			
Heart	3.1 ± 0.1	$2.9 \pm 0.3*$	$1.2 \pm 0.01^*$	$0.3 \pm 0.04^*$			
Spleen	0.9 ± 0.01	$1.1 \pm 0.1^*$	1.2 ± 0.02	$0.9 \pm 0.05^*$			
Kidney	4.2 ± 0.4	$8.2 \pm 0.6^*$	$5.6 \pm 0.3^*$	$2.3 \pm 0.06^*$			
Thyroid	0.8 ± 0.4	$1.2 \pm 0.6^*$	$2.7 \pm 0.3^*$	5.9 ± 0.06 *			
Urine	8.9 ± 0.4	15.4 ± 0.6 *	$20.7 \pm 0.3*$	40.1 ± 0.06 *			

Values represent mean ± SEM. * Means significantly differ from the previous each value using unpaired student's t-test (P<0.05).

Table 10. Biodistribution of ¹²⁵I-TP₅ in ascites bearing mice

Organs &		% ¹²⁵ I-TP ₅ /	gram organ			
Body fluids	Time post injection					
	15 min	30 min	60 min	180 min		
Ascites	3.50 ± 0.4	$5.7 \pm 0.6^*$	$7.6 \pm 0.3^*$	$5.8 \pm 0.06^*$		
Blood	16.1 ± 1.1	$12.5 \pm 0.2^*$	6.5 ± 0.04 *	$2.2 \pm 0.3^*$		
Bone	1.1 ± 0.05	$1.2 \pm 0.1^*$	$0.9 \pm 0.1^*$	$0.3 \pm 0.1^*$		
Muscle	1.3 ± 0.01	$2.3 \pm 0.02^*$	1.7 ± 0.1	$1.1 \pm 0.02^*$		
Liver	9.6 ± 0.05	$11.8 \pm 0.15^*$	$10.42 \pm 0.06^*$	3.9 ± 0.02		
Stomach	3.5 ± 0.9	6.2 ± 0.6	$9.1 \pm 0.16^*$	$2.3 \pm 0.2^*$		
Intestine	4.1 ± 0.50	$8.2 \pm 0.3^*$	$6.3 \pm 0.1^*$	$2.1 \pm 0.03^*$		
Lung	1.2 ± 0.1	$1.1 \pm 0.12^*$	$0.9 \pm 0.2^*$	$1.2 \pm 0.01^*$		
Heart	3.1 ± 0.8	$2.1 \pm 0.3^*$	$1.7 \pm 0.01^*$	$0.9 \pm 0.04^*$		
Spleen	0.8 ± 0.3	$0.9 \pm 0.1*$	0.7 ± 0.02	0.2 ± 0.05 *		
Kidney	6.1 ± 0.4	7.8 ± 0.6 *	$8.2 \pm 0.3*$	4.2 ± 0.06 *		
Thyroid	1.1 ± 0.4	2.3 ± 0.6 *	$3.1 \pm 0.3*$	4.1 ± 0.06 *		
Urine	4.3 ± 0.4	9.8 ± 0.6 *	$20.1 \pm 0.3*$	42.2 ± 0.06 *		

Values represent the mean \pm SEM, n=6 * Significantly different from the initial value of each organ using unpaired student's t-test (P<0.05)

Effect of reaction temperature. The labeling yield was optimal (87.5%) at ambient temperature, 25 °C and decreased by increasing temperature and this is may be due to the thermal decomposition of the ¹²⁵I-**TP**₅.³¹

Biodistribution of ¹²⁵I-TP₅ in normal mice. As cleared from Table 9, biodistribution study in mice showed that ¹²⁵I-TP₅ was distributed rapidly in blood, liver, intestine and kidney at 15 min post injection. After 30 min, ¹²⁵I-TP₅ uptake was significantly decreased in organs like blood. However, ¹²⁵I-TP₅ uptake was significantly increased in liver, kidney and intestine after 30 min. At 60 and 180 min post injection, the majority of tissues showed significant decrease in ¹²⁵I-TP₅ uptake. Thyroid gland showed significant increase in ¹²⁵I-TP₅ uptake at 6 and 180 min post injection.

Biodistribution of ¹²⁵I-TP₅ in ascites bearing mice.

The sites of greatest uptake of ¹²⁵I-**TP**₅ after 15 min post injection were the blood, liver, kidney and intestine (16%, 9.6%, 6% and 4.1%), respectively. Table 10 shows that the accumulation of ¹²⁵I-**TP**₅ was low in spleen, thyroid, bone and muscle at 15 min post injection. The uptake of ¹²⁵I-**TP**₅ in ascetic fluid was rapidly taking place as each mL of ascetic fluid received 3.5% of total activity. The uptake of ascetic fluid/mL was significantly increased at 30 and 60 min and reached 5.7% and 7.6%, respectively. Thyroid uptake was increased by time post injection mainly due to *in vivo* deiodination of ¹²⁵I-**TP**₅. ³² Urine uptake of ¹²⁵I-**TP**₅ increased with time, which confirms its excretion through renal pathway.

Table 11. Biodistribution of ¹²⁵I-**TP**₅ in solid tumor bearing mice.

Organs & body fluids	Percent I.D./gram organ Time post injection					
	15 min	30 min	60 min	180 min		
Blood	15.70 ± 1.10	12.02 ± 0.02*	7.9 ± 0.04*	4.95 ± 0.04*		
Bone	0.70 ± 0.01	$0.8 \pm 0.01^*$	$0.90 \pm 0.01^*$	$0.60 \pm 0.01^*$		
Control muscle	0.74 ± 0.01	$0.8 \pm 0.02^*$	0.560 ± 0.002	0.5 ± 0.002		
Tumor muscle	1.50 ± 0.01	$1.90 \pm 0.02^*$	1.960 ± 0.002	1.75 ± 0.002		
Liver	13.30 ± 0.5	$19.20 \pm 0.15^*$	$12.50 \pm 0.16^*$	$4.90 \pm 0.16^*$		
Lung	2.20 ± 0.10	$4.92 \pm 0.12^*$	$3.93 \pm 0.02^*$	$2.30 \pm 0.02^*$		
Heartw	6.05 ± 0.05	$4.51 \pm 0.05^*$	$2.50 \pm 0.01^*$	$1.20 \pm 0.01^*$		
Stomachw	4.80 ± 0.09	6.51 ± 0.30	$3.30 \pm 0.16^*$	$2.30 \pm 0.16^*$		
Intestine	3.5 ± 0.50	5.10 ± 0.30	$6.10 \pm 0.9^*$	$3.10 \pm 0.19^*$		
Kidney (urine)	6.90 ± 0.40	12.04 ± 0.60	$24.20 \pm 0.30^*$	$35.80 \pm 0.30^*$		
Spleen	0.90 ± 0.02	$1.60 \pm 0.04^*$	0.80 ± 0.02	0.50 ± 0.02		
Normal leg	1.80 ± 0.02	$3.60 \pm 0.04^*$	3.40 ± 0.02	2.20 ± 0.02		
Tumor leg	3.10 ± 0.40	8.04 ± 0.60	$9.90 \pm 0.30*$	8.10 ± 0.30 *		

Values represent mean \pm SEM, n=6 * Means significantly differ from the previous each value using unpaired student's t-test (p \leq 0.05).

Biodistribution of ¹²⁵I-TP₅ in solid tumor bearing mice. Table 11 shows the biodistribution of ¹²⁵I-TP₅ in important body organs and fluids in the solid tumor mice models at 15, 30, 60 and 180 min post injection. The amount of accumulated activity in left thigh tumor tissue was 3.1, 8.1, 9.9 and 8.1% at 15, 30, 60 and 180 min post injection, respectively. The maximum solid tumor uptake observed after 60 min post injection of ¹²⁵I-TP₅. Excretion of ¹²⁵I-TP₅ goes mainly through the kidney. The compound has shown that the decline of ¹²⁵I-TP₅ is slow from tumor site, which may be due to its interaction with DNA of tumor cells. These results showed that TP₅ may be potentially used as a radiopharmaceutical for tumor diagnosis when labeled with ¹²⁵I.

4. Conclusions

Trying to get a new anticancer drug, the thiopyrano[2,3-b] pyridine derivatives **4–9** were prepared starting from 2-mercapto-4,6-dimethylnicotinonitrile (1). The cytotoxicity activity of compounds 5, 6 and 8 was tested against MCF-7 and HCT-116 cell lines. The compound 5 showed dramatic effects against MCF-7 and HCT-116 cell lines, much better than 6 and 8. The compound 5 with potent inhibitory activity in tumor growth inhibition would be a potential anticancer agent. The incorporation of an Auger emitter (125I) into a tumor site was achieved by labeling of the compound 5 (TP₅) with ¹²⁵I. The appropriate conditions for synthesis of ¹²⁵I-TP₅ (87.5 % yield) are as follows: 75 μg of **TP**₅ as substrate, 50 μg of NBS as oxidizing agent, pH 4, room temperature, 15 min. High incorporation of 125I-TP5 in tumor sites (ascites tumor) facilitates tumor imaging. ¹²⁵I-**TP**₅ is convenient to transport ¹²⁵I to the nucleus of tumor cells. The decline of ¹²⁵I-**TP**₅ is slow from the tumor site and its excretion has been confirmed to go mainly through the renal pathway. The results showed that compound 5 (TP₅) may be potentially used as a radiopharmaceutical for tumor diagnosis when labeled with ¹²⁵I.

5. References

- J. Y. Zhang, Nat. Rev. Drug Discov. 2002, 1, 101–102. DOI:10.1038/nrd726
- G. S. Hassan, H. H. Kadry, S. M. Abou-Seri, M. M. Ali, A. E. E. Mahmoud, *Bioorg. Med. Chem.* 2011, 19, 6808–6817.
 DOI:10.1016/j.bmc.2011.09.036
- A. T. Taher, H. H. Georgey, H. I. El-Subbagh, Eur. J. Med. Chem.
 2012, 47, 445–451. DOI:10.1016/j.ejmech.2011.11.013
- A. I. Carmen, M. Carlos, Medicinal Chemistry of Anticancer Drugs, 1st ed.; Elsevier: Amsterdam, The Netherlands, 2008; pp. 1–8.
- 5. E. Borowski, M. M. Bontemps-Gracz, A. Piwkowska, *Acta Biochim. Pol.* **2005**, *52*, 609–627.
- 6. J.-K. Son, L. X. Zhao, A. Basnet, P. Thapa, R. Karki, Y. Na, Y.

- Jahng, T. C. Jeong, B.-S. Jeong, C.-S. Lee, E.-S. Lee *Eur. J. Med. Chem.* **2008**, *43*, 675–682. **DOI**:10.1016/j.ejmech.2007.05.002
- A. G. Amr, M. M. Abdulla, Bioorg. Med. Chem. 2006, 14, 4341–4352. DOI:10.1016/j.bmc.2006.02.045
- A. D. Settimo, A. M. Marini, G. Primofiore, F. D. Settimo, S. Salerno, C. L. Motta, G. Pardi, P. L. and Ferrarini, *J. Heterocy-cl. Chem.* 2000, *37*, 379–382. DOI:10.1002/jhet.5570370224
- P. L. Ferrarini, C. Mori, M. Badwanch, V. Galderone, R. Greco, C. Manera, A. Martinelli, P. Nieva, G. Saccomanni, *Eur. J. Med. Chem.* 2000, *35*, 815.
 DOI:10.1016/S0223-5234(00)00173-2
- T. Al. Nakibl, V. Bezjakl, M. J. Meeganz, Eur. J. Med. Chem. 1990, 25, 455–462. DOI:10.1016/0223-5234(90)90010-Z
- D. Prithwiraj, B. Michel, L. Delphine, *Bioorg. Med. Chem.* 2010, 18, 2537–2548. DOI:10.1016/j.bmc.2010.02.041
- 12. K. Bimal, B. Indrani, F. Frederick, *Eur. J. Med. Chem.* **2010**, *45*, 846–848. **DOI:**10.1016/j.ejmech.2009.11.024
- G. Damia, M. D'Incalci, Eur. J. Cancer 2009, 45, 2768–2781.
 DOI:10.1016/j.ejca.2009.08.008
- Y. Zheng, Z. Ma, X. Zhang, N. Yang, G. Yang, *Int. J. Chem.* 2011, 3(1), 42. DOI:10.5539/ijc.v3n1p42
- K. M. Dawood, J. Heterocycl. Chem. 2005, 42, 211–225.
 DOI:10.1016/j.wavemoti.2005.02.002
- M. A. Waly, I. I. EL-Hawary, W. S. Hamama, H. H. Zoorob, J. Heterocycl. Chem. 2013, 50, E12–E17.
 DOI:10.1002/jhet.1020
- W. S. Hamama, M. A. Waly, I. I. EL-Hawary, H. H. Zoorob, J. Heterocycl. Chem. 2016, 53, 953–957. DOI:10.1002/jhet.1631
- 18. M. A. Waly, I. I. EL-Hawary, T. M. El-gogary, *Med. Chem. Res.* **2013**, *22*, 1674–1678. **DOI:**10.1007/s00044-012-0161-4
- J. Mester, K. De Goeij, M. Sluyser, Eur. J. Cancer, 1996, 32, 1603. DOI:10.1016/0959-8049(96)00117-7
- A. Abd El-Bary, A. M. Amin, A. El-Wetery, S. Saad, M. Shoukry, *Pharmacol. Pharm.* 2012, 3, 97–102.
 DOI:10.4236/pp.2012.31014
- 21. A. M. Amin, S. E. Soliman, H. A. El-Aziz, S. Abo-El Enein, *Int. J. Chem.*, **2014**, *6*(*1*), 17–25. **DOI**:10.5539/ijc.v6n1p17
- D. L. Bailey, D. W. Townsend, P. E. Valk, M. N. Maisey, "Positron Emission Tomography: Basic Sciences". Secaucus, NJ: Springer-Verlag London. 2005, 62(5), 779–784.
 DOI:10.1007/b136169
- C. H. Cheng, C. F. Meares, D. A. Goodwin, In; "Application of nuclear and radiochemistry", (R. M. Lambrecht, N. Morcos, Eds.), Pergamon, New York, 1983, p. 103–114.
 DOI:10.1016/B978-0-08-027544-4.50016-2
- K. M. El-Azony, J. Radioanal. Nucl. Chem. 2010, 285, 315–320. DOI:10.1007/s10967-010-0583-8
- N. Greenwood, A. Earnshaw, Origin of the elements, isotopes and atomic weighs. In: "Chemistry of the Elements". Second Edition, Elsevier Ltd. Oxford, 1997, pp: 1–20.
 DOI:10.1016/B978-0-08-030712-1.50004-1
- K. M. El-Azony, A. A. El-Mohty, H. M. Killa, U. Seddik, S. I. Khater, *J. Labelled Comp. Radiopharm.*, 2009, 52(1), 1–5.
 DOI:10.1002/jlcr.1556
- I. T. Ibrahim, M. A. Motaleb, K. M. Attalah, J. Radioanal. Nucl. Chem. 2010, 285, 431–436. DOI:10.1007/s10967-010-0607-4

- L. L. Johnson, L. Schofield, T. Donahay, P. J. Mastrofranceso, J. Nucl. Med. 2000, 41(7), 1237–1243.
- 29. B. Johannsen, H. Spies: "Chemistry of Radiopharmacology of Technetium Complexes", Workshop on generator and cyclotron produced radiopharmaceuticals, Riyad, Saudi Arabia, Oct. 1991, 13–31.
- 30. P. Krogsgaard-Larsen, T. Liljefors, U. Madsen, Radiotracers:
- Synthesis and use in imaging. In: *Textbook of Drug Design and Discovery, Third Edition*, **2003**, 205–232.
- M. A. Motaleb, M. T. El-Kolaly, H. M. Rashed, A. Abd El-Bary J. Radioanal. Nucl. Chem. 2012, 292, 629–635.
 DOI:10.1007/s10967-011-1499-7
- M. A. Motaleb, M. E. Moustapha, I. T. Ibrahim, J. Radioanal. Nucl. Chem. 2011, 289(7), 239–245.
 DOI:10.1007/s10967-011-1069-z

Povzetek

Iz nikotinonitrilnih derivatov 1 smo lahko sintetizirali nove tiopirano[2,3-*b*]piridine 4–9. Citotoksično aktivnost izbranih spojin 5, 6 in 8 smo testirali na celičnih linijah MCF-7 in HCT-116. Spojina 5 (TP₅) je izkazala opazno inhibitorno aktivnost in je bila najbolj učinkovita, bolj kot spojini 6 in 8. Spojina 5, z močno inhibitorno aktivnostjo na rast tumorjev, bi lahko bila potencialna protirakava učinkovina. V luči naših rezultatov smo pripravili ¹²⁵I-radiooznačeno spojino 5 (¹²⁵I-TP₅) in preučili njeno citotoksičnost proti ascitnim tumorjem pri miših. Rezultati kažejo, da je spojina 5 (TP₅) potencialno uporabna kot radiofarmacevtska spojina za diagonozo tumorjev, kadar je označena s ¹²⁵I.



Except when otherwise noted, articles in this journal are published under the terms and conditions of the Creative Commons Attribution 4.0 International License